Journal of Power Sources 195 (2010) 8097–8103

Contents lists available at ScienceDirect

Journal of Power Sources

journal homepage: www.elsevier.com/locate/jpowsour

Generalized predictive control for fractional order dynamic model of solid oxide fuel cell output power

Zhonghua Deng[a], Hongliang Cao[a,*], Xi Li[a,*], Jianhua Jiang[a], Jie Yang[b,c], Yi Qin[a]

[a] Department of Control Science and Engineering, Key Laboratory of Education Ministry for Image Processing and Intelligent Control, Huazhong University of Science and Technology, Wuhan 430074, China
[b] School of Materials Science and Engineering, State Key Laboratory of Material Processing and Die and Mould Technology, Huazhong University of Science and Technology, Wuhan 430074, China
[c] School of Mechanical and Electronic Information, China University of Geosciences, Wuhan 430074, China

ARTICLE INFO

Article history:
Received 17 May 2010
Received in revised form 16 July 2010
Accepted 20 July 2010
Available online 30 July 2010

Keywords:
Solid oxide fuel cells
Generalized predictive control
Fractional order dynamic model
Forgetting factor recursive least squares

ABSTRACT

An adaptive generalized predictive control (GPC) system is presented for the management of output power of solid oxide fuel cells (SOFCs). The dynamics of SOFC output power are characterized by a fractional order model, which is more accurate than an integer order model to depict the dynamics; the fractional order dynamic model is taken as the controlled plant of the GPC system. The GPC algorithm adopts a linear approximation method that uses a linear predictive model to approximate locally and dynamically the nonlinear dynamics of SOFC output power at each sampling period. Moreover, the parameters of the predictive model are identified online to overcome the time-varying dynamics of SOFC output power via introducing a forgetting factor recursive least squares (FFRLS) algorithm. Finally, according to the future power outputs predicted by the predictive model, an optimal current control sequence is obtained by solving a multistage cost function. The results demonstrate that the dynamic responses of the GPC system are quick and smooth, and the change of the current control sequence is slow and smooth. The quick and smooth dynamics are important for satisfying the rapid load following of SOFC generating systems and for prolonging the lifetime of SOFC stack.

1. Introduction

Solid oxide fuel cells (SOFCs) generate directly electrical energy out of hydrocarbon fuels with a number of advantages, such as high electrical efficiency, fuel flexibility, low emissions, and quiet operation. Therefore, SOFC generating systems are emerging as a promising alternative in practical application, for domestic, commercial and industrial sectors [1,2].

However, the development of SOFCs is still facing some challenging problems, such as a longer lifetime and an elevated performance, towards its large-scale commercialization. In order to achieve these, an effective control system is required to ensure the safety and to satisfy the load demand during the operation of SOFCs [3–7].

The design of the control system of SOFCs is a difficult task, as a SOFC generating system is a nonlinear and time-varying system [2,8,9]. For nonlinear and time-varying systems, nonlinear model predictive control (NMPC) is a powerful optimized control approach. In NMPC, a predictive model is used to predict the future outputs of controlled plant on the basis of past inputs, outputs and future control sequences. The optimal control sequence is obtained by solving a nonlinear optimization problem. The nonlinear optimization problem is the key for the implementation of NMPC algorithms [3,10–12].

The application of NMPC algorithms in the field of fuel cells has been reported in many literatures. Wu et al. [9] developed a NMPC algorithm based on a radial basis function (RBF) neural network nonlinear model to control SOFC stack terminal voltage. The nonlinear optimization problem was solved by a golden mean method. Zhang et al. [3] designed a NMPC method for a SOFC system where the optimization method was an iterative algorithm with convergence criterion fulfilled. Yang et al. [13,14] built a NMPC algorithm based on a Takagi–Sugeno (T–S) fuzzy model to online control the stack temperature of SOFCs. The optimal control sequence was obtained by a branch-and-bound method that is a kind of iterative searching algorithm in a discrete search space of tree structure. Similar NMPC algorithms were also applied to molten carbonate fuel cells (MCFCs) and proton exchange membrane fuel cells (PEMFCs) [15,16]. Golbert and Lewis [17] presented a NMPC method to satisfy power demands robustly based on a simplified physical model in a PEMFC system; the nonlinear optimization problem was also solved by an iterative method.

* Corresponding author. Tel.: +86 027 87540924; fax: +86 027 87540924.
E-mail addresses: chlhzust@hotmail.com (H. Cao), lixi_wh@126.com (X. Li).

0378-7753/$ – see front matter © 2010 Elsevier B.V. All rights reserved.
doi:10.1016/j.jpowsour.2010.07.053

Nomenclature

C_{dl}	double layer capacitance in triple phase boundary, F cm^{-2}
E_o	open circuit voltage, V
i	current density, A cm^{-2}
I	unit matrix
k	index of discrete time
M	control horizon
n	number of single cells or order of fractional order capacitance
n_a	order of controlled variable
n_b	order of control variable
N	maximum costing horizon
P	output power of SOFC stacks, W
R_e	electrolyte resistance, Ω cm^2
R_t	activation resistance, Ω cm^2
s	Laplace operator
S	available area of single cells, cm^2
T	matrix transpose
T_s	sampling period
T_{ref}	response time of exponential function in reference trajectory
z	forward shift operator
z^{-1}	back shift operator

Greek letters

α	a small enough number
β	a large enough number
λ	control weighting sequence
ρ	forgetting factor

Subscripts

a	anode
c	cathode
dl	double layer
e	electrolyte
o	open
r	reference trajectory
rat	rated
ref	reference
t	activation
1	associated with anode
2	associated with cathode

As the iterative processes for solving nonlinear optimization problems are time consuming and expensive, there is still difficulty in the implementation of the aforementioned NMPC algorithms in practical application. In order to implement NMPC algorithms in practical systems, it is important to reduce the computation time. To avoid the nonlinear optimization problem, Jurado [18] adopted a Hammerstein model for the design of NMPC systems to online control the output voltage of SOFCs. As the linear dynamic block of the Hammerstein model is a remaining part of the predictive model, the optimization can be completed by quadratic programming. Similar method was also applied to the control of SOFC output voltage [19]. Zhang and Gang [11] used a T–S fuzzy model to represent approximately the nonlinear dynamics of SOFCs. Since the fuzzy model approximates locally and dynamically the nonlinear dynamics by a set of linear models at each sampling period, linear model predictive control (MPC) theory can be used easily to design an offset-free fuzzy MPC for the load following of SOFCs. Vahidi et al. [20] proposed a MPC design for the optimal distribution of current demands between the power sources in a PEMFC-ultracapacitor system. The nonlinear plant was linearized around operating points; the computation burden was alleviated extraordinarily. Li et al. [21] adopted a least squares support vector machines (LS-SVM) method to build a nonlinear off-line model of the operating temperature of a PEMFC stack. During the operation of the PEMFC, the off-line model was linearized at each sampling period, and a generalized predictive control (GPC) method was used to online control the plant. Since the explicit solution of the GPC algorithm can be obtained, its computation burden is greatly alleviated. Therefore, the implementation of GPC algorithms is feasible, and the GPC algorithm is also suitable for the control of output power of SOFCs with slight alterations.

In this research, an adaptive GPC algorithm is presented for the control of output power of SOFCs. The dynamics of SOFC output power is greatly complex, for the electrochemical process occurring at the triple phase boundary (TPB) is a time-varying and nonlinear process [2,22]. It is difficult to characterize accurately the complex electrochemical process via an integer order capacitance in the transient equivalent circuit of the inherent impedance of SOFCs. However, the electrochemical process can be depicted more accurately by a fractional order capacitance or a constant phase element (CPE) [22–26]. Therefore, a fractional dynamic order model is used to characterize the dynamics of SOFC output power; it has been performed in our previous study [25]. Moreover, the fractional order model is modified by adding white Gaussian noise to take into account the influences from some disturbance factors, such as stack temperature, inlet flow rates, and inlet pressure.

Taking the fractional order dynamic model as the controlled plant, we investigate the design of the GPC system. A method of linear approximation is adopted in the GPC system; the method makes use of a linear predictive model to approximate locally and dynamically the fractional order dynamic model at each sampling period. Moreover, the parameters of the predictive model are identified online by introducing a forgetting factor recursive least squares (FFRLS) algorithm so that the nonlinear and time-varying dynamics of SOFC output power is predicted accurately. Based on the predicted power outputs, an optimal current control sequence is obtained by solving a multistage cost function; the output power of SOFCs is adjusted according to the optimal current control signal. The dynamic responses of the GPC system are quick and smooth, which is useful for satisfying the rapid load following of SOFC generating systems and for prolonging the lifetime of SOFC stack.

2. Generalized predictive control system of SOFC output power

The structure of the GPC system of SOFC output power is shown in Fig. 1. The GPC system is aimed at controlling the output power of the SOFC stack, $y(k)$, by manipulating the current, $u(k)$. The current control sequence derives from a predictive controller by optimizing

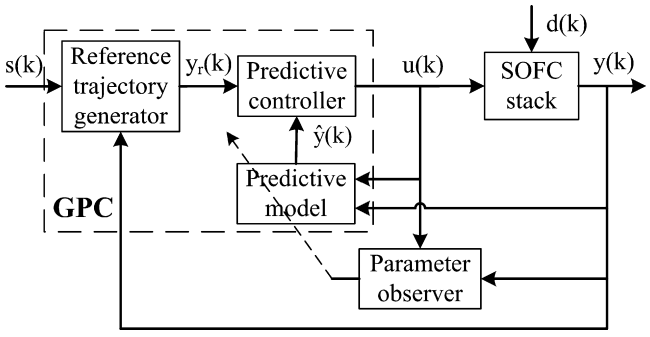

Fig. 1. Structure of an adaptive generalized predictive control system of SOFC output power.

a cost function. The optimization process is completed in such a way that the future power output, $\hat{y}(k)$, is driven close to the reference trajectory, $y_r(k)$. The future power outputs are predicted by means of a predictive model. The parameters of the predictive model are estimated online by a parameter observer at each sampling period. The reference trajectory is computed via a reference trajectory generator taking into account the power set-point sequence, $s(k)$, and the output power at current instant k. The components of the GPC system are presented in detail in the following sections.

2.1. Developing fractional order dynamic model of output power of SOFC stack

The fractional order dynamic model of output power of SOFC stack is developed with an assumption that the electrical characteristics are consistent for all single cells in the stack. The fractional order dynamic model of single cells has been performed in our previous study [25]. The output voltage of single cells can be represented in the form of,

$$u(t) = E_o - u_a(t) - u_c(t) - R_e i(t), \tag{1a}$$

where $u_a(t)$ and $u_c(t)$ are the overvoltages on the anode and cathode of single cells respectively,

$$u_a(t) = L^{-1}\left[\frac{R_{ta}I(s)}{1+R_{ta}C_{dla}s^{n_1}}\right], \tag{1b}$$

$$u_c(t) = L^{-1}\left[\frac{R_{tc}I(s)}{1+R_{tc}C_{dlc}s^{n_2}}\right]. \tag{1c}$$

All the variables in Eqs. (1a), (1b) and (1c) have the same definition as ones in Ref. [25].

Therefore, the fractional order dynamic model of output power of SOFC stack can be obtained by,

$$P(t) = u(t) \times i(t) \times S \times n, \tag{2}$$

where S is the available area of single cells, and n is the number of single cells in stack. Considering Eqs. (1a), (1b), and (1c), Eq. (2) can be written as:

$$P(t)=Sn\left\{E_o-L^{-1}\left[\frac{R_{ta}I(s)}{1+R_{ta}C_{dla}s^{n_1}}\right]-L^{-1}\left[\frac{R_{tc}I(s)}{1+R_{tc}C_{dlc}s^{n_2}}\right]-R_e i(t)\right\} i(t). \tag{3}$$

For Eq. (3), the key of numerical evaluation is the calculation of the overvoltages of anode and cathode, which is described in detail in Appendix A.

In addition, the fractional order dynamic model, Eq. (3), was developed in the case of constant work conditions: constant stack temperature, constant inlet flow rates, and constant inlet pressure. Practically, the changes of those factors will result in corresponding changes of the dynamics of SOFC output power [2]. Therefore, taking into account the influences from those factors, we add white Gaussian noise to the dynamic model in order to simulate the electrical characteristics in practical SOFC generating systems. For instance, white Gaussian noises with signal-to-noise ratio 50 dB are added to the model parameters (consisting of R_{ta}, C_{dla}, n_1, R_{tc}, C_{dlc}, n_2, R_e).

2.2. Generalized predictive control

In this section, an adaptive GPC algorithm is designed taking the fractional order dynamic model developed above as the controlled plant. The GPC algorithm was proposed by Clarke et al. [27]. It makes use of a Controlled Auto-Regressive Integrated Moving Average (CARIMA) model to predict the system dynamics. The predictive model is a linear model, which has no promising precision to predict the future outputs of a nonlinear and time-varying system; the precision plays a decisive role in the controller [10]. For the accurate prediction of the nonlinear and time-varying dynamics, the GPC system presented in the research adopts a method of linear approximation that makes use of the linear CARIMA model to approximate locally and dynamically the system at each sampling period; the parameters of the CARIMA model are identified online using a FFRLS algorithm, which will be presented in Section 2.3.

The CARIMA model is described by,

$$A(z^{-1})y(k) = B(z^{-1})u(k-1) + \frac{c(z^{-1})\omega(k)}{\Delta}, \tag{4a}$$

where, $u(k)$ and $y(k)$ are the control and controlled sequences of the system, $\omega(k)$ is a zero mean white noise, z^{-1} is a back shift operator, and Δ is difference operator,

$$\Delta = 1 - z^{-1}. \tag{4b}$$

$A(z^{-1})$, $B(z^{-1})$, and $c(z^{-1})$ are the following polynomials:

$$A(z^{-1}) = 1 + a_1 z^{-1} + \cdots + a_{n_a} z^{-n_a}, \tag{4c}$$

$$B(z^{-1}) = b_0 + b_1 z^{-1} + \cdots + b_{n_b} z^{-n_b}, \tag{4d}$$

$$c(z^{-1}) = c_0 + c_1 z^{-1} + \cdots + c_{n_c} z^{-n_c}. \tag{4e}$$

For simplicity, the $c(z^{-1})$ polynomial is chosen to be 1 [10].

In the GPC method, an optimal control sequence is computed by minimizing a multistage cost function,

$$J = E\left\{\sum_{j=1}^{N}(\hat{y}(k+j) - y_r(k+j))^2 + \sum_{j=1}^{M}\lambda(j)(\Delta u(k+j-1))^2\right\}, \tag{5}$$

where $E\{\cdot\}$ is the expectation operator, N is the maximum costing horizon, M is the control horizon, $\lambda(j)$ is a control weighting sequence, $\hat{y}(k+j)$ is an optimum ahead prediction of the system output at $(k+j)$th instant, $y_r(k+j)$ is the future reference trajectory at $(k+j)$th instant.

In Eq. (5), the increments of the control sequences are taken into account over the control horizon, and the weight of those increments can be set commodiously. Therefore, the multistage cost function is useful for the control of the change of current drawn from the stack.

In order to optimize the cost function, the optimal prediction, $\hat{y}(k+j)$, can be obtained by considering the following Diophantine equations:

$$1 = E_j(z^{-1})A(z^{-1})\Delta + z^{-j}F_j(z^{-1}), \tag{6a}$$

$$E_j(z^{-1})B(z^{-1}) = G_j(z^{-1}) + z^{-j}H_j(z^{-1}). \tag{6b}$$

Here, $E_j(z^{-1})$, $F_j(z^{-1})$, $G_j(z^{-1})$, and $H_j(z^{-1})$ are the following polynomials:

$$E_j(z^{-1}) = e_0 + e_1 z^{-1} + \cdots + e_{j-1} z^{-j+1}, \tag{6c}$$

$$F_j(z^{-1}) = f_0^j + f_1^j z^{-1} + \cdots + f_{n_a}^j z^{-n_a}, \tag{6d}$$

$$G_j(z^{-1}) = g_0 + g_1 z^{-1} + \cdots + g_{j-1} z^{-j+1}, \tag{6e}$$

$$H_j(z^{-1}) = h_0^j + h_1^j z^{-1} + \cdots + h_{n_b-1}^j z^{-n_b+1}. \tag{6f}$$

It is simple to obtain the above polynomials by computing the Diophantine equations recursively [27].

If Eq. (4a) is multiplied by $\Delta E_j(z^{-1})z^j$, we have

$$E_j(z^{-1})A(z^{-1})\Delta y(k+j)=E_j(z^{-1})B(z^{-1})\Delta u(k+j-1)+E_j(z^{-1})\omega(k+j). \tag{7}$$

Considering Eqs. (6a) and (6b), we can write Eq. (7) in the following,

$$y(k+j) = G_j(z^{-1})\Delta u(k+j-1) + F_j(z^{-1})y(k) + H_j(z^{-1})\Delta u(k-1) + E_j(z^{-1})\omega(k+j). \quad (8)$$

Therefore, $\hat{y}(k+j)$ is obtained,

$$\hat{y}(k+j)=G_j(z^{-1})\Delta u(k+j-1)+F_j(z^{-1})y(k)+H_j(z^{-1})\Delta u(k-1), \quad (9)$$

for the reason that $\omega(k+j)$ is a zero mean white noise.

The selection about the reference trajectory, $y_r(k+j)$, is an important aspect for the dynamics of the GPC system. In order to obtain a good dynamic performance that the output value can be driven to the set-point trajectory quickly and smoothly, we choose the following reference trajectory [28],

$$y_r(k+j) = s(k+j) - (s(k) - y(k))\exp\left(\frac{-T_s}{T_{ref}}\right), \quad (10)$$

where $s(k+j)$ is the set-point trajectory at$(k+j)$th instant, T_s is the sampling period, and T_{ref} defines the speed of response. The reference trajectory approaches the set-point trajectory exponentially, which is in favor of the rapidity and stability of the GPC system.

For the convenience of computing the optimal control sequence, we re-write the cost function, Eq. (5), in a vector form,

$$J = E\left\{(\mathbf{y}-\mathbf{y_r})^T(\mathbf{y}-\mathbf{y_r}) + \lambda\mathbf{u}^T\mathbf{u}\right\}, \quad (11a)$$

where

$$\mathbf{y} = [y(k+1), \ldots, y(k+N)]^T, \quad (11b)$$

$$\mathbf{y_r} = [y_r(k+1), \ldots, y_r(k+N)]^T, \quad (11c)$$

$$\mathbf{u} = [\Delta u(k), \ldots, \Delta u(k+M-1)]^T, \quad (11d)$$

$$\boldsymbol{\lambda} = \lambda\mathbf{I}. \quad (11e)$$

Making the gradient of J equal to zero, we can get the optimal control sequence,

$$\mathbf{u} = \left(\mathbf{G}^T\mathbf{G} + \lambda\mathbf{I}\right)^{-1}\mathbf{G}^T[\mathbf{y_r} - \mathbf{F}y(k) - \mathbf{H}\Delta u(k-1)]. \quad (12)$$

The control signal actually sent to the controlled plant is the first element of the vector $\mathbf{u}$, which is given by,

$$u(k) = u(k-1) + [\,1 \quad 0 \quad \cdots \quad 0\,]_{1\times M}\mathbf{u}. \quad (13)$$

2.3. Online parameter identification of CARIMA model

A FFRLS algorithm is adopted to identify the CARIMA model online [29]. Let us re-write Eq. (4a),

$$A(z^{-1})\Delta y(k) = B(z^{-1})\Delta u(k-1) + \omega(k). \quad (14)$$

Considering Eqs. (4c) and (4d), we rearrange Eq. (14) as following,

$$\Delta y(k) = -a_1\Delta y(k-1) - \cdots - a_{n_a}\Delta y(k-n_a) + b_0\Delta u(k-1) + b_1\Delta u(k-2) + \cdots + b_{n_b}\Delta u(k-n_b-1) + \omega(k). \quad (15)$$

Eq. (15) can be written in a vector form as,

$$\Delta y(k) = \varphi(k)^T\theta_0 + \omega(k), \quad (16a)$$

where $\varphi(k)$ is an information vector,

$$\varphi(k) = [-\Delta y(k-1), \ldots, -\Delta y(k-n_a), \Delta u(k-1), \times \Delta u(k-2), \ldots, \Delta u(k-n_b-1)]^T, \quad (16b)$$

Table 1
Parameters of the adaptive generalized predictive control system of SOFC output power.

Item	Value
Open circuit voltage, E_o	1.104 (V)
Available area of single cells, S	81 (cm^2)
Number of single cells, n	30
Rated power of the SOFC stack, P_{rat}	2000 (W)
Control weighting sequence, λ	7
Order of controlled variable, n_a	6
Order of control variable, n_b	6
Sampling period, T_s	0.01 (s)
Response time of exponential function in reference trajectory, T_{ref}	1.49 (s)
Forgetting factor, ρ	0.96

and θ_0 is the parameter vector to be identified,

$$\theta_0 = [a_1, \ldots, a_{n_a}, b_0, b_1, \ldots, b_{n_b}]^T. \quad (16c)$$

Let $\hat{\theta}(k-1)$ denote the estimate of θ_0 at instant $(k-1)$. Then, the one-step ahead prediction error at instant k can be defined to be,

$$\varepsilon(k) = \Delta y(k) - \varphi(k)^T\hat{\theta}(k-1). \quad (17)$$

Finally, the recursive relation of the parameter vector, θ_0, is described as following:

$$\hat{\theta}(k) = \hat{\theta}(k-1) + \frac{P(k-1)\varphi(k)\varepsilon(k)}{\rho + \varphi(k)^T P(k-1)\varphi(k)}, \quad (18a)$$

$$P(k) = \frac{1}{\rho}\left\{P(k-1) - \frac{P(k-1)\varphi(k)\varphi(k)^T P(k-1)}{\rho + \varphi(k)^T P(k-1)\varphi(k)}\right\}, \quad (18b)$$

where $\rho(0<\rho<1)$ is called the forgetting factor. $P(k)$ is a positive definite covariance matrix. Initial values of $\hat{\theta}(k)$ and $P(k)$ are given by,

$$\begin{cases}\hat{\theta}(-1) = \alpha 1_{n_a+n_b+1} \\ P(-1) = \beta^2 I\end{cases}. \quad (18c)$$

Here, α is a small real number, e.g. $\alpha = 10^{-15}$, β should be large enough, e.g. $\beta = 10^{10}$, $1_{n_a+n_b+1}$ is a (n_a+n_b+1) dimensional vector whose elements are 1, and I is an unit matrix of appropriate dimensions.

3. Results and discussion

The adaptive GPC system of SOFC output power designed above is implemented in this section. All the parameters of the GPC system, excepting the maximum costing and control horizons, are specified in Table 1.

3.1. Deciding the maximum costing and control horizons

The maximum costing and control horizons (N and M) are dominant model parameters for the performance of the GPC system. An initial value of M, $M=1$, gives generally acceptable control behavior according to the thumb-rules [27]. Therefore, under the condition of $M=1$, we can investigate the system performance, such as stability and rapidity, in the presence of different N. The performance under different N can be revealed by a step response test of the system.

The step responses of the GPC system with different N ($N=2$–6) are shown in Fig. 2, where the setting power is changed from 486 W to 1458 W at the instant of 2 s. In the light of the step responses, an important phenomenon can be found that the rapidity of the system increases with increasing N. But when N becomes too large, such as $N=5$ and 6, the dynamic performance of the system will be unsatisfying for the occurrence of phenomenon of oscillation. Especially, for the case of $N=6$, the overshoot and undershoot are

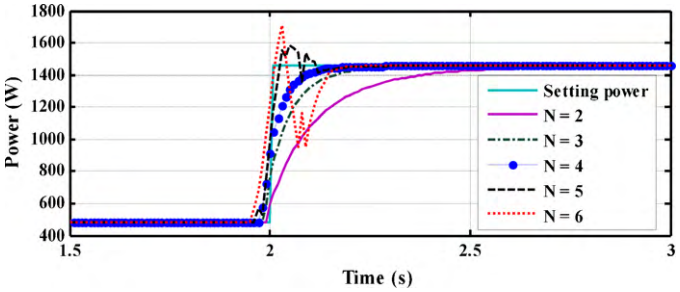

Fig. 2. Step responses of the adaptive generalized predictive control system of SOFC output power with different N in the case of $M = 1$.

as high as 17.01% and 34.98%, respectively. For the other three cases of $N = 2$–4, the system performance are satisfying for the dynamic process are smooth and stable. Taking into account the rapidity and stability, the maximum costing horizon is chosen with $N = 4$ in the GPC system.

Under the condition of $N = 4$, the system performance is also investigated for different M ($M = 1$–4) as shown in Fig. 3. For all the cases, the SOFC output power is driven to the setting power smoothly and quickly; the system rapidity decreases slightly with the increase of M (Fig. 3(a)). The rapidity is a critical performance index for a control system, but in some practical plants, such as a SOFC generating system, the increments of control sequences should be taken into account carefully.

In the control system of SOFC output power, the control sequence is the current drawn from the stack. When the current is drawn from the stack, heat will be generated due to electrochemical reactions occurring at the TPB and ohmic heat loss deriving from resistances to the flow of ions and electrons in the electrodes, electrolyte, and interconnects. The change of the current will lead to the fluctuation of operating temperature in stack; the stack temperature fluctuation will result in thermal stress, which is destructive for stack durability [30–33]. Therefore, the current should be changed smoothly to alleviate the produce of thermal stress in stack. In Fig. 3(b), the change of current density in the case of $M = 4$, is the smoothest of all the cases. So, considering the change behavior of

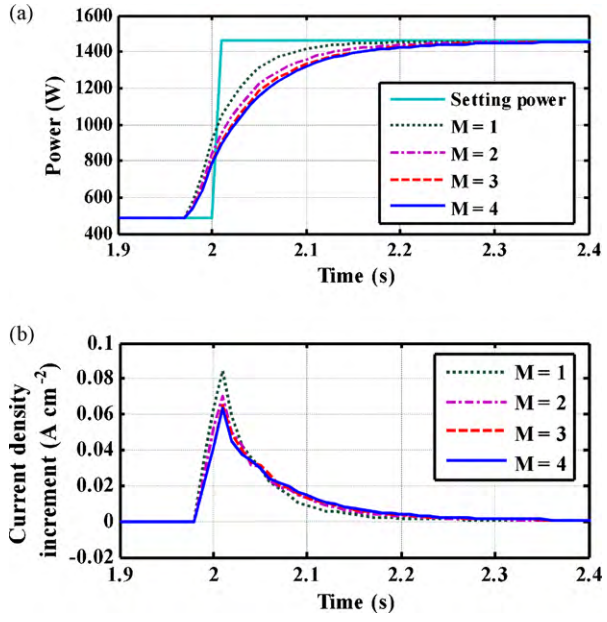

Fig. 3. Step responses of the adaptive generalized predictive control system of SOFC output power with different M in the case of $N = 4$: (a) dynamics of SOFC output power, (b) current density increments of the control current.

Table 2
A testing scenario for the adaptive generalized predictive control method consisting of several power demand set-points within the rated power of the SOFC stack.

Time instant (s)	Setting power density (W cm^{-2})	Setting power (W)
1	0.1	243
2	0.2	486
3	0.4	972
4	0.8	1944
5	0.7	1701
6	0.5	1215
7	0.1	243

current control sequences, the control horizon is chosen with $M = 4$ in the GPC system.

3.2. Testing adaptive generalized predictive control system of SOFC output power

The adaptive GPC system of SOFC output power is tested based on the model parameters decided above. The power demand set-points in the GPC system are set from 0.1 W cm^{-2} to 0.8 W cm^{-2}, where the highest value is smaller than the rated power density, 0.835 W cm^{-2}. In addition, the changes of the set-points keep a relation of geometric series during the rise and drop processes of the power demand set-points; the detailed testing scenario is listed in Table 2.

On the basis of the power demand set-points in Table 2, the dynamic responses of the adaptive GPC system of SOFC output power are shown in Fig. 4. The efficiency of the adaptive GPC method is illustrated by the fact that the SOFC output power is driven to the trajectory quickly and smoothly. By analyzing the performance indexes of the dynamic responses, it can be found that the SOFC output power reaches the power demand set-points without oscillation, overshoot, and offset, and the rise-time is less than 0.5 s

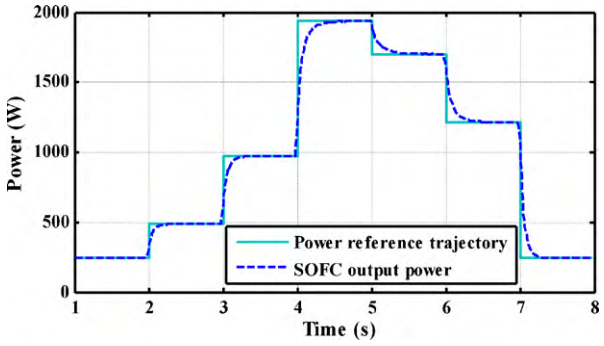

Fig. 4. Dynamic responses of the adaptive generalized predictive control system of SOFC output power.

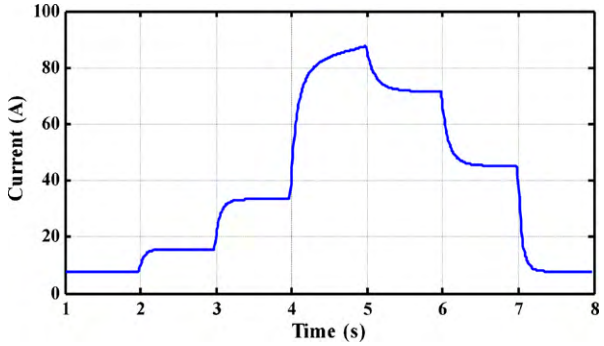

Fig. 5. Control current computed by the adaptive generalized predictive control algorithm.

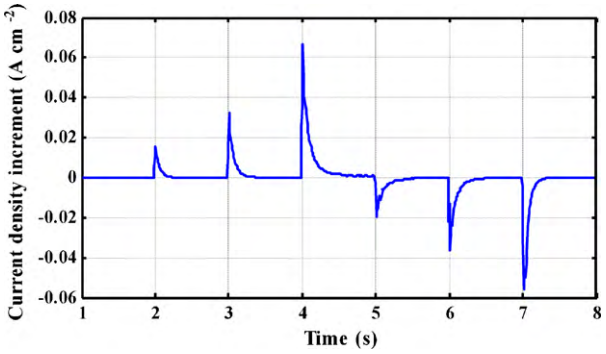

Fig. 6. Current density increments of the control current.

at all step change set-points. Therefore, the adaptive GPC method is capable for the control of the SOFC output power.

Furthermore, Fig. 5 demonstrates that the current control sequence for the above dynamic responses changes smoothly. For instance, the maximum value of current density increments is less than 0.07 A cm^{-2} (Fig. 6). The smooth current control sequence is very effective to alleviate thermal stress in stack. Therefore, the adaptive GPC method considering the change behavior of the current is valuable for maximizing stack durability.

4. Conclusions

An adaptive generalized predictive control system is designed for the management of SOFC output power in this research. The dynamic responses of the control system are quick and smooth, which is a solid foundation for the load following of SOFC generating systems. Moreover, the smooth current control sequence supports the usefulness of the control system to maintain the thermal stress in stack within a safe operating range. In future work, it is valuable to study the synchronous management of the electrical and heat energy of SOFC generating systems.

Acknowledgments

This research was financially supported by National Science Foundation of China (60804031), the "863" High-Tech Project (2006AA05Z148), and the Foundation of the Key Laboratory of Education Ministry for Image Processing and Intelligent Control, PR China (200701). At the same time, I would like to thank Chris Dyer, Editor, Journal of Power Sources, and anonymous reviewers for their help and constructive suggestions.

Appendix A. Appendix A. Calculation of electrode overvoltages

Step 1: The transfer function of the electrode

The transfer function of an electrode (anode or cathode) can be expressed in the light of Eqs. (2b) and (2c),

$$\frac{U_x(s)}{I(s)} = \frac{R_t}{1 + R_t C_{dl} s^n}, \tag{A.1}$$

where $U_x(s)$ denotes the Laplace transform of the overvoltage of the electrode $u_x(t)$. Eq. (A.1) can be re-written,

$$\frac{U_x(s)}{I(s)} = \frac{a}{s^n + b}, \tag{A.2}$$

with $a = 1/C_{dl}$, $b = 1/(R_t C_{dl})$.

Step 2: The fractional differential equation of the electrode

Eq. (A.2) can also be written in the following:

$$s^n U_x(s) + b U_x(s) = a I(s). \tag{A.3}$$

The inverse Laplace transform applied to Eq. (A.3), the following fractional differential equation is obtained [34,35]:

$${}_0D_t^n u_x(t) + b u_x(t) = a i(t). \tag{A.4}$$

Step 3: Discretization of the fractional differential equation

According to the Grünwald-Letnicov (GL) definition [34], the discretization formula of fractional derivatives is defined to be,

$${}_0D_t^n u_x(t) = h^{-n} \sum_{j=0}^{k} \omega_j^n u_x(k-j), \tag{A.5}$$

where h is step size, which is equal to the sampling period in the GPC system; ω_j^n is the weight coefficient, which is calculated by the following recurrence equation,

$$\begin{cases} \omega_0^n = 1 \\ \omega_j^n = \left(1 - \dfrac{n+1}{j}\right) \omega_{j-1}^n, \quad j = 1, 2, 3, \ldots \end{cases}. \tag{A.6}$$

Eq. (A.5) can then be re-written in the form:

$${}_0D_t^n u_x(t) = h^{-n} u_x(k) + h^{-n} \sum_{j=1}^{k} \omega_j^n u_x(k-j). \tag{A.7}$$

Finally, the discretization fractional differential equation is obtained,

$$h^{-n} u_x(k) + h^{-n} \sum_{j=1}^{k} \omega_j^n u_x(k-j) + b u_x(k) = a i(k). \tag{A.8}$$

The electrode overvoltage $u_x(k)$ then is computed as following:

$$u_x(k) = \frac{a i(k) - h^{-n} \sum_{j=1}^{k} \omega_j^n u_x(k-j)}{h^{-n} + b}. \tag{A.9}$$

References

[1] S. Kaka, A. Pramuanjaroenkij, X.Y. Zhou, International Journal of Hydrogen Energy 32 (7) (2007) 761–786.
[2] J. Larminie, A. Dicks, Fuel Cell Systems Explained, 2nd ed., Chichester, England, John Wiley & Sons Ltd., 2003.
[3] X.W. Zhang, S.H. Chan, H.K. Ho, J. Li, G. Li, Z. Feng, International Journal of Hydrogen Energy 33 (9) (2008) 2355–2366.
[4] Y. Xie, X. Xue, in: Fourth Dubrovnik Conference, International Journal of Hydrogen Energy 34 (16) (2009) 6882–6891.
[5] M. Sorrentino, C. Pianese, Journal of Fuel Cell Science and Technology 6 (4) (2009) 41011–41012.
[6] C. Hongliang, X. Li, D. Zhonghua, Y. Qin, Modeling for Electrical Characteristics of Solid Oxide Fuel Cell Based on Fractional Calculus, IEEE, Guilin, China, 2009.
[7] M. Fardadi, F. Mueller, F. Jabbari, Journal of Power Sources 195 (13) (2010) 4222–4233.
[8] F. Jurado, Fuel Cells 5 (1) (2005) 105–114.
[9] X.J. Wu, X.J. Zhu, G.Y. Cao, H.Y. Tu, Journal of Power Sources 179 (1) (2008) 232–239.
[10] E.F. Camacho, C. Bordons, Model Predictice Control, Springer, Berlin, 1999.
[11] T.J. Zhang, F. Gang, IEEE Transactions on Fuzzy Systems 17 (2) (2009) 357–371.
[12] L. Magni, N.G. De, R. Scattolini, Automatica 37 (10) (2001) 1601–1607.
[13] J. Yang, X. Li, H.G. Mou, L. Jian, Journal of Power Sources 188 (2) (2009) 475–482.
[14] J. Yang, X. Li, H.G. Mou, L. Jian, Journal of Power Sources 193 (2) (2009) 699–705.
[15] F. Yang, X. Zhu, G. Cao, W. Hu, Journal of Power Sources 183 (1) (2008) 253–256.
[16] X. Li, Z. Deng, G. Cao, X. Zhu, D. Wei, Journal of Central South University of Technology 13 (6) (2006) 722–725.
[17] J. Golbert, D.R. Lewin, Journal of Power Sources 135 (1–2) (2004) 135–151.
[18] F. Jurado, Journal of Power Sources 158 (1) (2006) 245–253.
[19] H.B. Huo, X.J. Zhu, W.Q. Hu, H.Y. Tu, J. Li, J. Yang, Journal of Power Sources 185 (1) (2008) 338–344.

[20] A. Vahidi, A. Stefanopoulou, H. Peng, American Control Conference 1 (30) (2004) 834–839.
[21] X. Li, G. Cao, X. Zhu, Energy Conversion and Management 47 (7–8) (2006) 1032–1050.
[22] M.E. Orazem, B. Tribollet, Electrochemical Impedance Spectroscopy, John Wiley & Sons, Inc., Hoboken, NJ, 2008.
[23] N. Fouquet, C. Douleta, G.D. Nouillanta, B. Ould-bouamamab, Journal of Power Sources 159 (2) (2006) 905–913.
[24] E.T. Mcadams, A. Lackermeier, J.A. Mclaughlin, D. Macken, J. Jossinet, Biosensors and Bioelectronics 10 (1–2) (1995) 67–74.
[25] H. Cao, Z. Deng, X. Li, J. Yang, Y. Qin, International Journal of Hydrogen Energy 35 (4) (2010) 1749–1758.
[26] S. Westerlund, IEEE Transactions Dielectrics and Electrical Insulation 1 (5) (1994) 826–839.
[27] D.W. Clarke, C. Mohtadi, P.S. Tuffs, Automatica 23 (2) (1987) 137–148.
[28] J.M. Maciejowski, Predictive Control with Constraints, Prentice Hall, 2000.
[29] D. Feng, C. Tongwen, IEEE Transactions on Circuits and Systems I: Regular Papers 52 (3) (2005) 555–566.
[30] T.X. Ho, P. Kosinski, A.C. Hoffmann, A. Vik, International Journal of Hydrogen Energy 35 (9) (2010) 4276–4284.
[31] Z. Qu, P.V. Aravind, N.J. Dekker, A.H. Janssen, N. Woudstra, A.H. Verkooijen, Journal of Power Sources 195 (23) (2010) 7787–7795.
[32] K.P. Recknagle, R.E. Williford, L.A. Chick, D.R. Rector, M.A. Khaleel, Journal of Power Sources 113 (1) (2003) 109–114.
[33] Y. Inui, N. Ito, T. Nakajima, A. Urata, Energy Conversion and Management 47 (15–16) (2006) 2319–2328.
[34] I. Podlubny, Fractional Differential Equations, Academic Press, San Diego, 1999.
[35] Y. Chen, B.M. Vinagre, I. Podlubny, Nonlinear Dynamics 38 (1) (2004) 155–170.